catalysts

MDPI

Article

Catalytic Activity of Ni Based Materials Prepared by Different Methods for Hydrogen Production via the Water Gas Shift Reaction

Opas Tojira and Pannipa Tepamatr *

Department of Chemistry, Faculty of Science and Technology, Thammasat University, Khlong Luang 12120, Thailand
* Correspondence: p.tepamat@gmail.com

Abstract: Water gas shift reactions (WGS) were evaluated over Ni/CeO_2 and Ni/CeSmO catalysts for hydrogen production. The effects of catalyst preparation method and Sm loading were investigated. The Ni/ceria and Ni/CeSmO catalysts were synthesized by combustion, sol gel and sol gel-combustion method. After WGS tests, the catalysts were determined the carbon deposition by thermogravimetric analysis. The thermogravimetric analysis and temperature programmed NH_3 desorption showed that addition of Sm promoter made higher the weak acid sites and lower the amount of carbon deposition than the unpromoted catalyst due to it being easily removed. CO chemisorption result indicated that Ni/Ce5%SmO catalyst prepared by combustion method has the highest Ni metal dispersion and metallic surface area compared to the other catalysts. The enhancement of WGS activity of this catalyst is due to more surface active sites being exposed to reactants. Furthermore, H_2-temperature programmed reduction analysis confirmed an easiest reduction of this catalyst. This behavior accelerates the redox process at the ceria surface and enhances the oxygen vacancy concentration. The catalytic activity measurements exhibited that the optimum Sm loading was 5% wt. and the best catalyst preparation was the combustion method. The high surface area and small crystallite size of the 5%Ni/Ce5%SmO (combustion) catalyst resulted in sufficient dispersion, which closely related to the WGS activity of the catalyst.

Keywords: hydrogen production; Sm; water gas shift; Ni; ceria

Citation: Tojira, O.; Tepamatr, P. Catalytic Activity of Ni Based Materials Prepared by Different Methods for Hydrogen Production via the Water Gas Shift Reaction. *Catalysts* **2023**, *13*, 176. https://doi.org/10.3390/catal13010176

Academic Editors: Vincenzo Vaiano and Olga Sacco

Received: 27 November 2022
Revised: 26 December 2022
Accepted: 29 December 2022
Published: 12 January 2023

1. Introduction

H_2 is considered as a prominent energy carrier in modern green chemicals. Water gas (or syngas) is a mixture of CO and H_2 which is considered to be an alternative to conventional fuels in various applications. Hydrogen can be combusted similarly to natural gas, used as fuel for fuel cells, or converted into other hydrocarbon fuels. The water gas shift (WGS) reaction is applied in the syngas cleaning to remove carbon monoxide and produce hydrogen along with carbon dioxide before using a syngas product stream for a wide range of applications. The water gas shift process is a moderately exothermic and reversible reaction which controls relative content of hydrogen and carbon oxides in the product stream:

$$CO + H_2O \rightleftharpoons CO_2 + H_2 \ \Delta H = -41.2 \text{ kJ/mol} \quad (1)$$

The WGS reaction is quite sensitive to temperature and increasing the temperature shifts to reactants. Due to the reversible process of the WGS reaction, the forward reaction rate is greatly inhibited by reaction products. Generally, the maximum CO conversion and selectivity are controlled by the equilibrium state. However, the kinetic potential of the catalyst has a great influence on the actual reaction rate of the desired products. It depends on the feed stream and the catalyst characteristics.

The water gas shift operation conditions and the nature of the metal phase and support influenced the catalytic performance. There is strong evidence that the oxide-supported

catalyst is directly involved in the water gas shift mechanism. CeO_2-based catalysts are very attractive because of their high oxygen storage capacity, mobility and reducibility. CeO_2 supported Pt catalysts are the most active for WGS reaction but economically not feasible [1,2]. Ni/ceria-based catalysts are promising materials due to their high WGS activity and low cost. This outstanding behavior is linked to the content of active metal, the metal dispersion, the metal-support interaction and the composition of the support [3–5]. Moreover, mixed oxides have received much attention in water gas shift reaction due to their excellent performance which is attributed to oxygen vacancy formation. A recent study found that CeO_2/TiO_2 supported gold catalysts presented better water gas shift activity than either of the individual oxide counterparts [6]. This result was due to the higher concentration of oxygen vacancy in mixed oxide catalysts which facilitates the limiting step of water gas shift reaction. Many studies have focused on the enhancement of oxygen vacancy concentration by doping metal ions with different oxidation states into the oxide, thus producing oxygen vacancies for charge compensation [7–9]. For example, Ayesha A et al. [10] found that doping Cu and Sm into CeO_2 increased the CO oxidation activity by about 64% compared to that of pure ceria. Additionally, they discovered that Cu^{2+} and Sm^{3+} dopants were located in the nearest neighbor sites of oxygen vacancy which reveals that more oxygen defects were generated with doping Cu and Sm. G. Avgouropoulos et al. demonstrated that doping Sm^{3+} into CeO_2 increases the dispersion of Au species on the metal oxide support. The doping of Sm improves the catalytic performance of Au/CeO_2 catalyst in the preferential CO oxidation reaction [11]. Moreover, the preparation methods of the catalysts have influence on the properties of CeO_2-based materials, such as crystallite phase, surface area, particle size, catalytic activity and solubility limit of dopants in CeO_2 [12]. Various synthesis methods are reported for the preparation of ceria-based solid solutions such as co-precipitation [13,14], sol gel [15] and combustion method [16,17]. Recently, Ni/CeO_2 was synthesized by the sol-gel method and compared with the Ni/CeO_2 catalyst prepared by impregnation method [18]. The catalysts performance was investigated in the dry reforming of methane. Ni/CeO_2 prepared by sol-gel method improved the resistance to sintering and reduced the carbon formation rates during the methane dry reforming reaction. These results were due to the stronger metal support interaction and greater amount of oxygen vacancies.

This work reveals the development of more simple methods to prepared ceria based materials with high performance for water gas shift reaction (including combustion, sol gel and sol gel-combustion method). The effect of Sm doped-ceria over Ni/CeO_2 catalyst on the water gas shift performance was also investigated. The Ni/ceria based catalysts were evaluated in different temperature and Sm loading (0, 5, 10, 15 wt.%). The physicochemical properties of the catalysts were studied by BET surface area, X-ray diffraction, Raman spectroscopy, H_2-Temperature programmed reduction, temperature programmed NH_3 desorption, chemisorption technique and thermogravimetric techniques. The results of the physicochemical characterization were discussed in correlation to the exhibited WGS performance of the supported Ni catalysts.

2. Experimental Procedure

2.1. Catalysts Preparation

The catalyst preparation process is based on a redox reaction between a fuel (an organic compound) and an oxidant (metal nitrate) which generates the exothermicity essential for nucleation and growth of the metal oxide powder. Urea (NH_2CONH_2) is used as fuel to ignite the reaction [19,20]. Additionally, urea is a complexing agent for a number of metal ions because it contains the amino group at the end [21].

Ceria and samarium doped ceria supports were synthesized by combustion, sol gel and sol-gel combustion method. For combustion method [22,23], $Ce(NO_3)_3{\cdot}6H_2O$ (Sigma-Aldrich Pte. Ltd., Singapore) and $Sm(NO_3)_3{\cdot}6H_2O$ (Sigma-Aldrich Pte. Ltd., Singapore) were used as starting materials for the preparation of pure ceria and cerium-samarium oxide supports. They were mixed with urea using the stoichiometry between oxidant and

urea is 2.5:1. The mixed reactant was dissolved with deionized water and heated by Bunsen burner until an auto-ignition occurred. Heating at high temperature caused decomposition of nitrate and other organic compounds. Therefore, the final product will be CeO_2 and CeSmO mixed oxide. In order to study the effect of percent Sm loaded into the support, various amounts of Sm were varied as 0, 5, 10 and 15 wt.% which is denoted as CeO_2, Ce5%SmO, Ce10%SmO and Ce15%SmO, respectively.

For samples preparation procedure by sol gel method, the mixtures of $Ce(NO_3)_3{\cdot}6H_2O$, $Sm(NO_3)_3{\cdot}6H_2O$ and urea were dissolved with deionized water. NH_3 solution was dropped into the mixed solution to adjust the pH 10 under constant agitation using a magnetic stirrer at 300 rpm and 80 °C. After 2 h of mixing, the obtained gel was dried at 100 °C for 24 h and followed by calcination at 450 °C for 4 h in an ambient atmosphere.

The procedure for the preparation of Sm-doped ceria by sol gel-combustion method is a combination of the combustion and sol gel method. The mixtures of $Ce(NO_3)_3{\cdot}6H_2O$, $Sm(NO_3)_3{\cdot}6H_2O$ and urea were dissolved with deionized water. NH_3 solution was dropped into the mixed solution to adjust the pH 10 under constant agitation using a magnetic stirrer at 300 rpm and 80 °C. After 2 h of mixing, a homogenous solution was heated by Bunsen burner until an auto-ignition occurred.

Impregnation method was used for the preparation of Ni catalysts. Nickel (II) nitrate hexahydrate (Alfa Aesar, Thermo Fisher Scientific Inc, Seoul, South Korea) was dissolved in minimal amount of DI water. The salts solution of nickel was added to CeO_2 and Sm-doped ceria supports. All samples were dried overnight at 100 °C and calcined at 650 °C for 8 h.

2.2. Catalyst Characterization

Pore size and specific surface area of the samples were measured with BELSORP-MAX instrument. The catalysts were treated under vacuum at 300 °C for 3 h before the measurement. The specific surface areas of all samples were determined by N_2 adsorption-desorption isotherms at 77 K in the relative pressures range of 0.05–0.3.

X-ray power diffraction pattern of all samples was operated at 0.02° per step and 0.5 s per step over a 2θ range of 20–80° with the current of 40 mA and 40 kV using an X'Pert Pro diffractometer (PANalytical). Nickel-filtered Cu K_α radiation was used to collect the X-ray diffractograms. The full width at half maximum of the strongest (111) reflection was considered for the calculation of the CeO_2 crystallite size from Scherrer's formula.

The Raman spectra of Ni/ceria and Ni/Ce5%SmO prepared by combustion method were performed using Perkin Elmer System 2000 FTIR/FT-Raman. Ar ion laser irradiation was used to collect the Raman spectra in the range of 200–1000 cm^{-1} with an output power of 10 mW and wavelength of 532 nm.

H_2-Temperature Programmed Reduction (H_2-TPR) measurement was employed to study the reduction behavior of the catalysts from a catalysts analyzer BELCAT-B. Prior to a TPR experiment, the catalyst was treated under high purity helium at 120 °C for 30 min. A mixture of 5%H_2 and argon was utilized for TPR experiments operating from 40 °C to 1000 °C with the rate of 10 °C/min. During the reduction of the catalyst, the H_2 consumption was determined by thermal conductivity detector (TCD).

The acid sites of the catalysts were investigated by temperature programmed NH_3 desorption. First, a mixed gas of 10% NH_3 in helium was adsorbed by the reduced catalysts at 50 °C for 1 h. Then, the excessive unadsorbed NH_3 was cleaned with a flow of He for 1 h. After that, the sample was heated to 500 °C with a heating rate of 10 °C/min under He flow. The NH_3 desorption curve was plotted as a function of temperature.

Thermogravimetric analysis of the used catalysts was conducted on by an integrated thermal analyzer (STA 449C) from 300 to 800 °C with heating rate of 10 °C/min under 30 mL/min of air atmosphere.

The metal surface area and metal dispersion were calculated from the total gas chemisorption using a mixture of 10% carbon monoxide and helium carrier gas. All samples were reduced with hydrogen at 400 °C for an hour. After cooling with helium, CO chemisorption pulse was operated under the flow of 10% CO/He at 50 °C at the rate of

30 mL/min. The flow of CO out from the reactor was monitored by thermal conductivity detector.

Amount of adsorption per 1 g of sample (V_m, cm^3/g^{-1})

$$V_m = V_{chem}/m \quad (2)$$

% Metal dispersion (D)

$$D = V_{chem}/22{,}414 \times SF \times MW \times 100/c \quad (3)$$

Metal weight (c, g)

$$c = m \times p/100 \quad (4)$$

Metal surface area (surface area of metal per 1 g of sample) (Am, m^2/g)

$$Am = V_{chem}/22{,}414 \times SF \times 6.02 \times 10^{23} \times \sigma_m \times 10^{-18}/m \quad (5)$$

where V_{chem}: amount of adsorption/cm^3, m: sample weight/g, MW: metal atomic weight/$gmol^{-1}$, SF: stoichiometry factor, p: weight percentage of supported metal content/wt%, σ_m: cross-section area of one metal atom/nm^2.

2.3. Water Gas Shift Activity

The performance of the water gas shift reaction was studied in the temperature range of 100–500 °C. About 150 mg of the catalysts were placed in a stainless steel fixed bed flow reactor between two layers of quartz wool. Prior to the water gas shift activity measurement, the prepared catalyst was reduced by heating in 5% H_2/N_2 balanced gas from room temperature to 400 °C and maintaining at this temperature for 1 h. The tube furnace was used to control the temperature of the reactor. For WGS activity testing, H_2O was fed through a pre-heater using a syringe pump. The feed gas contained 5% CO, 10% H_2O and 85% N_2. The gas mixtures of carbon monoxide and nitrogen were fed into the reactor with water vapor. Preliminary measurements were operated to consider proper conditions from which internal and external mass transfer effects are not dominant. When considering the effect of external mass transfer, the particle size diameter of the catalysts was between 100–200 μm in all testing. Furthermore, the total flow rate was kept constant at 100 mL min^{-1} in all experiments. Reaction products were analyzed by an on-line Shimadzu GC-14B gas chromatography equipped with thermal conductivity detector and a Unibeads C column. The catalytic activities of water gas shift reaction can be calculated by the formula:

$$\%COconversion = \frac{CO_{in} - CO_{out}}{CO_{in}} \times 100 \quad (6)$$

3. Results and Discussion

3.1. Catalysts Characterization

Figure 1 presents the X-ray diffraction profiles of the synthesized catalysts. The formations of ceria phases with fluorite-type cubic crystal structure were found in all samples which corresponded well to JCPDS no. 43-1002 of standard ceria. In addition, the diffraction peaks of NiO crystalline phase were found at around 2θ = 37.3°, 43.4° and 63.2° for 5%Ni/$CeO_{2(combustion)}$, 5%Ni/Ce5%SmO $_{(sol\ gel)}$ and 5%Ni/Ce5%SmO $_{(sol\ gel\text{-}combustion)}$. However, the absence of reflection peak of NiO in 5%Ni/Ce5%SmO $_{(combustion)}$ indicates that NiO is highly dispersed on the ceria surface.

The physical characteristics of supported Ni catalysts were showed in Table 1. The specific surface area was determined by using multipoint Brunauer-Emmett-Teller (BET) method. The pore volume and mean pore diameter were obtained by applying the Barrett-Joyner-Halenda (BJH) method. As is clear, the enhancement of the Sm amount from 5 to 15 wt.% led to a decrease of the surface area of catalysts from 54 to 29 m^2/g, respectively. It should be noted that a partial destruction and blockage of some micropores on the support

surface were due to the increase of the Sm content. Hence, reducing of pore volume of the catalyst leads to lowering of catalyst surface area. In addition, larger pore diameter when higher Sm content indicates that Sm moves to occupy pore area and may block up small pores underneath. This in turn resulted in reduction of surface area. On the other hand, Sm^{3+} in 5%Ni/Ce5%SmO prepared by combustion method stabilizes the support and can prevent the support from the sintering by maintaining small crystallite size and high surface area.

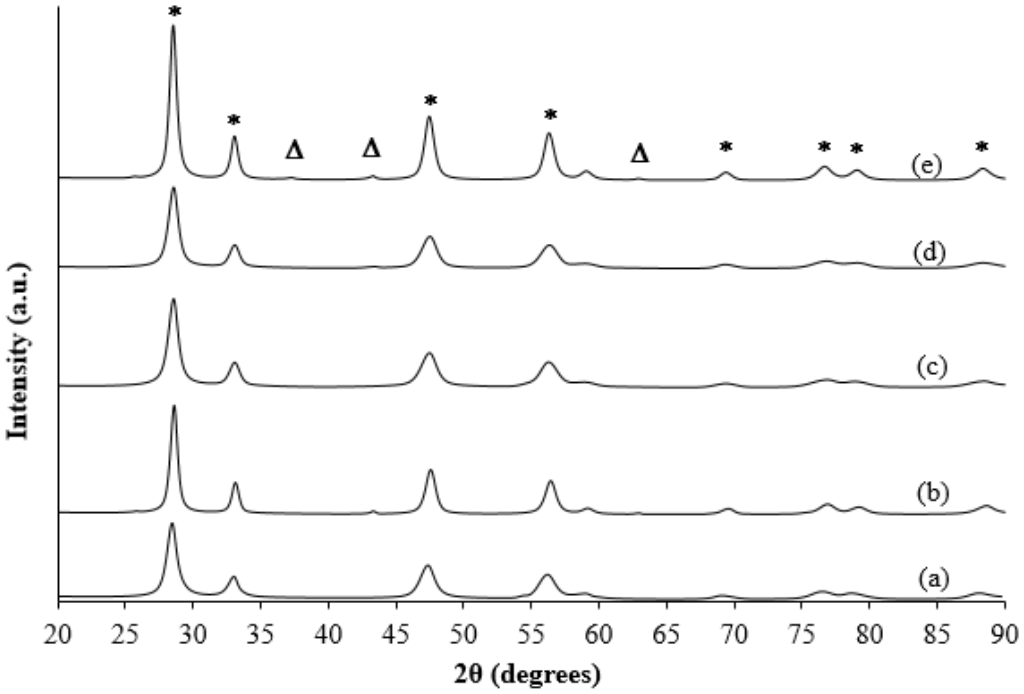

Figure 1. XRD patterns of Ni catalysts, (**a**) CeO_2(combustion), (**b**) 5%Ni/CeO_2(combustion), (**c**) 5%Ni/Ce5%SmO(combustion), (**d**) 5%Ni/Ce5%SmO(sol gel-combustion) and (**e**) 5%Ni/Ce5%SmO(sol gel). * CeO_2 JCPDS 43-1002, Δ NiO JCPDS 75-0197.

Table 1. BET surface area, average pore diameter and total pore volume of Ni-based catalysts prepared by different methods.

Catalysts	BET Surface Area [a] (m^2/g)	Total Pore Volume [a] (cm^3/g)	Average Pore Diameter [a] (nm)	Crystallite Size [b] (nm)
5%Ni/CeO_2(combustion)	29	0.06	8.35	13.35
5%Ni/Ce5%SmO(combustion)	54	0.08	5.88	9.01
5%Ni/Ce10%SmO(combustion)	34	0.06	6.96	9.55
5%Ni/Ce15%SmO(combustion)	29	0.05	7.51	10.44
5%Ni/Ce5%SmO(sol gel)	46	0.08	7.24	13.41
5%Ni/Ce5%SmO(sol gel-combustion)	48	0.08	6.78	11.32

[a] Estimated from N_2 adsorption at −196 °C; [b] Calculated from the 111 diffraction peak broadening.

Defect structures of ceria, 5%Ni/ceria and 5%Ni/Ce5%SmO prepared by combustion method were investigated by Raman spectroscopy (Figure 2). All catalysts present a Raman peak at about 460 cm^{-1} which is assigned to the F_{2g} mode of the cubic fluorite crystal structure of ceria. In 5%Ni/Ce5%SmO catalyst, F_{2g} mode exhibits a systematic shift to lower energies. Such a decrease in energy is consistent with dilatation of unit cell parameter due to the incorporation of large Sm^{3+} ions in cerium lattice. Moreover, there is another

broad peak at around 550–650 cm^{-1}. It indicates the presence of a surface defect of doping cations which is related to oxygen vacancies evolution [24].

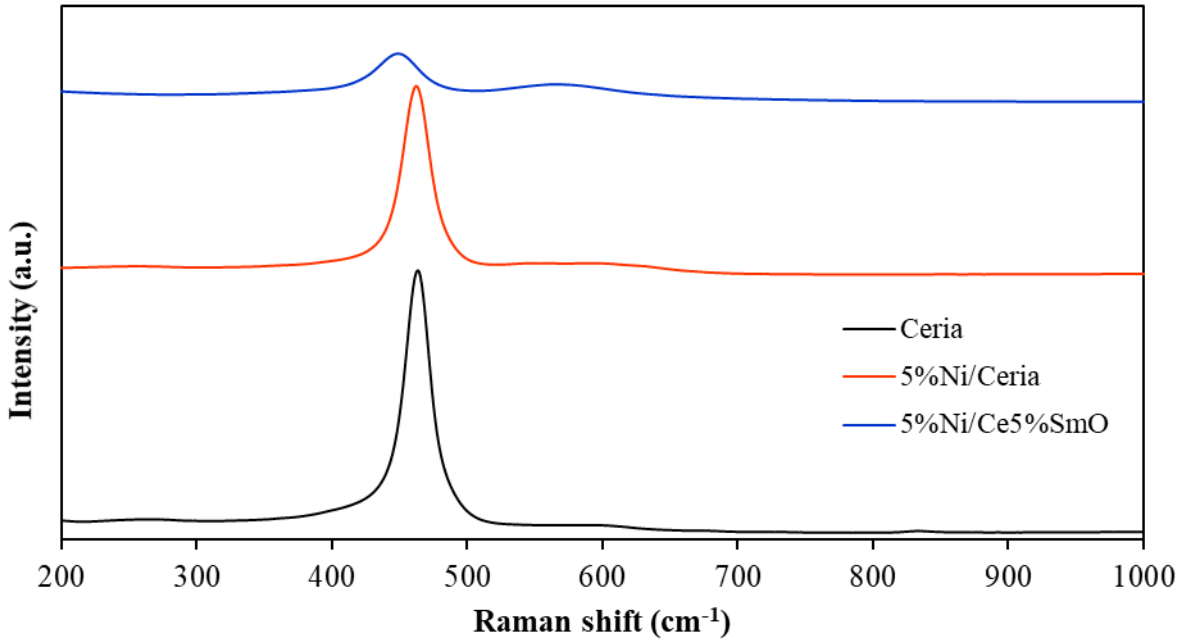

Figure 2. Raman spectra of ceria, 5%Ni/ceria and 5%Ni/Ce5%SmO prepared by combustion method.

The TPR profiles of 5%Ni/CeO_2 and 5%Ni/Ce5%SmO (Figure 3) catalysts prepared by different methods are characterized by a low-temperature peak at 260–280 °C, medium temperature features located at 350–370 °C and the bulk reduction at 850 °C. The consumption peak at low temperature is attributed to reduction of NiO species [25–27]. The peak at medium temperature is attributed to the Ni−catalyzed reduction of the surface shell of ceria [28,29]. The H_2−TPR of 5%Ni/Ce5%SmO (Figure 3) prepared by combustion method exhibited two NiO reduction peaks at 260 °C and 290 °C which indicated a different environment of Ni. The peak at 260 °C is similar to the reduction peak of Ni in the vicinity of ceria while the peak at 290 °C is probably due to the present of Sm. The NiO reduction peak of 5%Ni/Ce5%SmO prepared by combustion method appeared at the lowest temperature when compared with 5%Ni/Ce5%SmO prepared by sol gel and sol gel-combustion method. Figure 4 displays the H_2−TPR profiles of Ni/ceria and Ni/CeSmO prepared by combustion method with different wt.% of Sm. It is interesting to note that addition of 5%Sm to ceria support prepared by combustion method shifts the reduction temperature of NiO species from 275 °C to 260 °C. The result indicates that 5%Ni/Ce5%SmO catalysts should be more active than 5%Ni/ceria. Addition of Sm^{2+}/Sm^{3+} at higher contents (10 wt.% and 15 wt.%) does not improve the reducibility and this is probably due to aggregation of SmO_x particles. The H_2−TPR of 5%Ni/Ce15%SmO prepared by combustion method is different from those of other catalysts. Only one reduction peak at high temperature of this catalyst is due to a concurrent reduction of NiO species and surface ceria. The reduction temperature of 5%Ni/Ce5%SmO catalyst prepared by combustion method is the lowest. Generally, the oxygen vacancies formation leads to the exchange of oxygen easily. Therefore, reactive oxygen species can be produced and easily reduced by hydrogen at a low temperature. Combined with the result of Raman spectra, it was found that the presence of the oxygen vacancies improves the reduction of solid solutions.

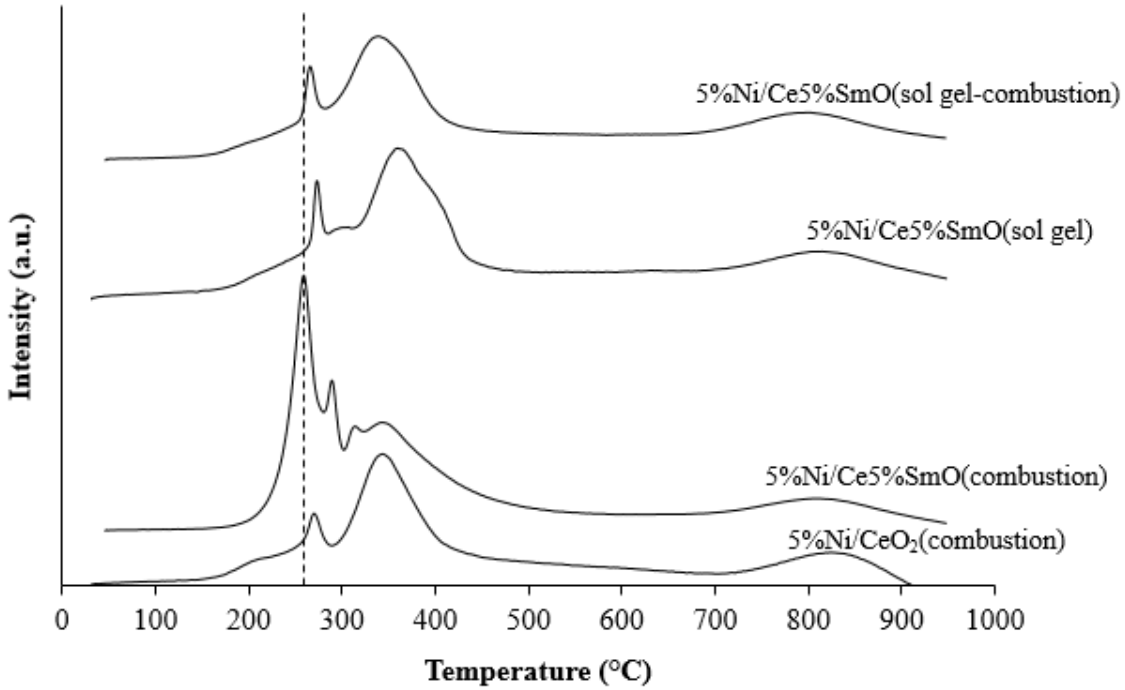

Figure 3. H_2-TPR profiles of supported Ni catalysts prepared by different methods.

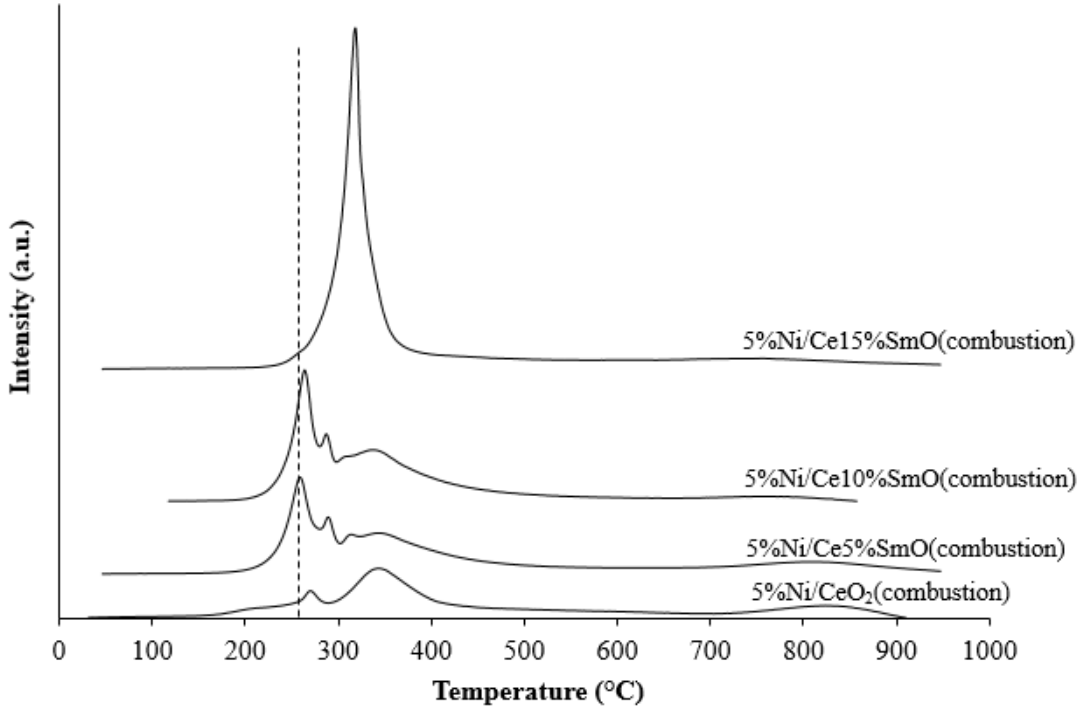

Figure 4. H_2-TPR profiles of supported nickel catalysts prepared by combustion method under different samarium loading.

A dispersion of Ni over Ni/CeO_2 and Ni/CeSmO prepared by different method and Sm loading was studied by CO chemisorption analysis (Table 2). It was found that Sm addition to Ni/CeO_2 enhances the dispersion of Ni metal on the catalyst surface. However, the increase of Sm amount to 15 wt.% leads to lowering of Ni metal dispersion. This result is probably due to aggregation of Sm at high content. Moreover, metallic Ni was believed to be active sites for the water gas shift reaction. The influence of Sm addition on metallic

Ni surface area was investigated which revealed that 5%Ni/Ce5%SmO catalyst prepared by combustion method has the highest Ni surface area of 1.25 m^2/g. Generally, higher metallic surface area of the catalysts provides an increase in WGS activity, as more surface active sites are exposed to reactants [30].

Table 2. The surface area and dispersion of metallic Ni prepared by different methods.

Catalysts	Ni Dispersion [c] (%)	Ni Surface Area [c] (m^2/g)
5%Ni/CeO_2(combustion)	0.12	0.84
5%Ni/Ce5%SmO(combustion)	0.19	1.25
5%Ni/Ce10%SmO(combustion)	0.15	0.98
5%Ni/Ce15%SmO(combustion)	0.10	0.68
5%Ni/Ce5%SmO(sol gel)	0.13	0.85
5%Ni/Ce5%SmO(sol gel-combustion)	0.14	0.89

[c] Estimated from CO-chemisorption.

3.2. Catalyst Evaluation

Figure 5 illustrates %CO conversion of Ni/CeO_2 and Ni/Ce5%SmO prepared by different methods. For Ni/CeO_2(combustion), the conversion started above 200 °C and rises up slowly to reach the maximum of 90% conversion at 350 °C. Among all the catalysts, 5%Ni/Ce5%SmO(combustion) exhibited the best water gas shift activity with the highest CO conversion of 99% at 350 °C. This result agrees nicely with the H_2-TPR profile which indicates that Ni/Ce5%SmO(combustion) is easiest to be reduced.

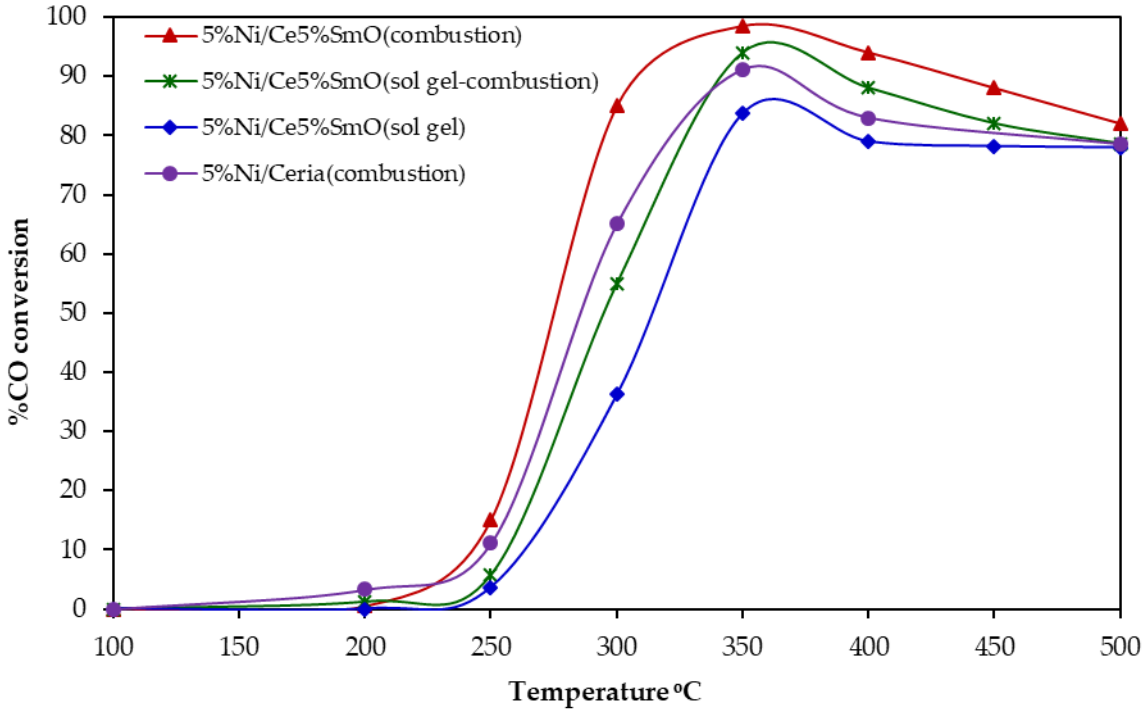

Figure 5. Water gas shift activity of supported Ni catalysts.

In water gas shift reaction, CH_4 is an undesired product because the decomposition of CH_4 may generate carbon which poisons the catalyst. The loss of WGS activity due to carbon formation causes blockage of the catalyst active sites and the loss of effective surface area [31]. Figure 6 shows CH_4 and CO_2 yield as a function of temperature. The amount of CH_4 decreases when the temperature increases from 300 to 500 °C. Ni/Ce5%SmO catalyst had less CH_4 production cause the reduction of coke formation. On the other hand, the

CO_2 yield increased with rising temperature. Maximum CO_2 yield was found at around 350 °C and then the CO_2 yield decreased if the temperature was further increased. At higher temperature, there is no methanation, and the water gas shift reaction increases the CO_2 concentration. However, the reduction of CO_2 yield was due to the reverse water gas shift reaction when the temperature was further increased.

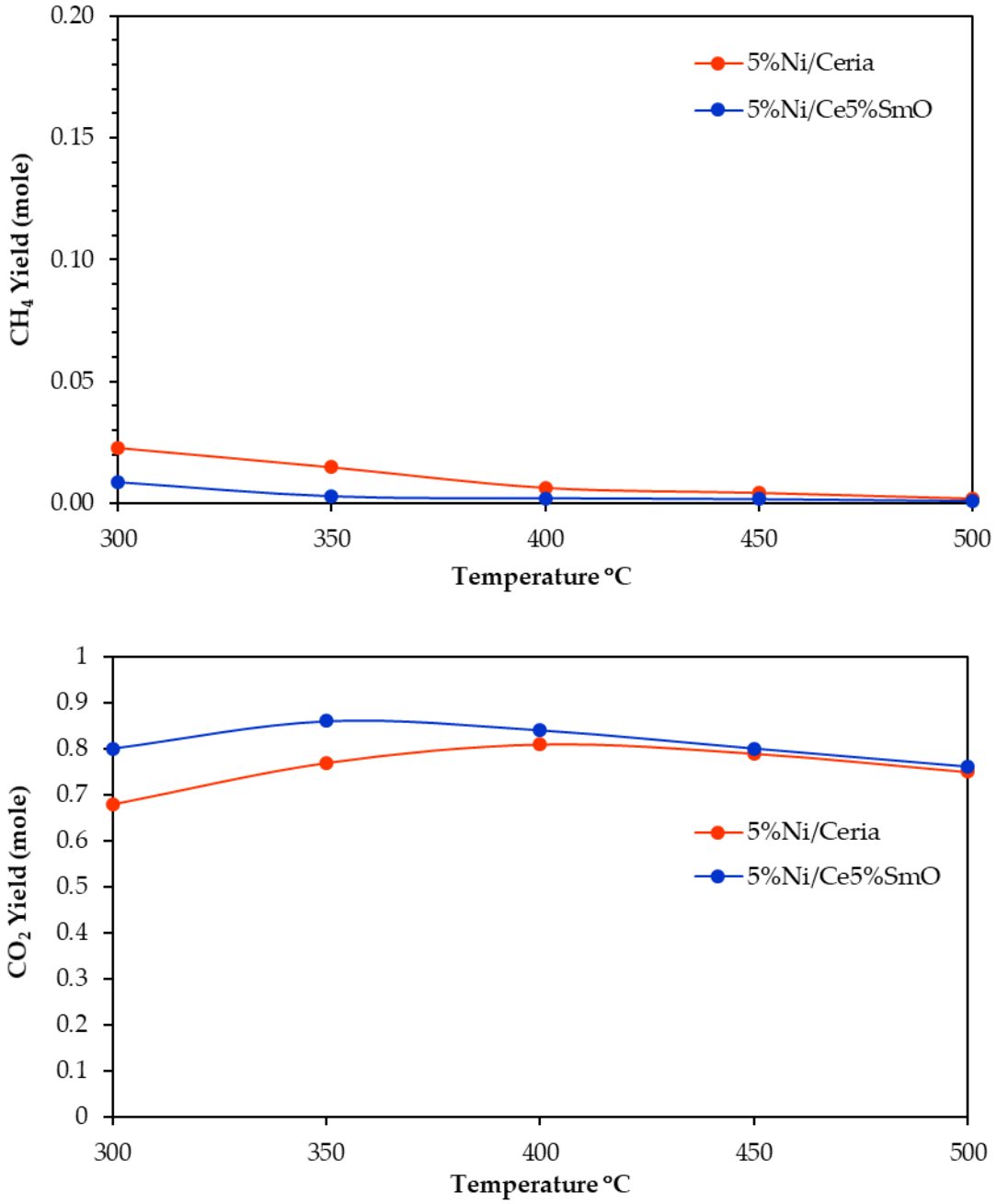

Figure 6. The effect of temperature on the CO_2 and CH_4 yield of water gas shift reaction.

The WGS reaction stability of Ni/CeO_2 and Ni/Ce5%SmO prepared by the combustion method was tested at 280 °C under the feed gas composition of 5%CO, 10% H_2O and balance N_2. As shown in Figure 7, the conversion of $5\%Ni/CeO_2$ decreased from 47% to 36% after 60 h of the water gas shift reaction test whereas 5%Ni supported on Ce5%SmO mixed oxide support retains a high water gas shift stability for the whole period of 60 h. Therefore, the addition of Sm improved both WGS activity and stability of the Ni catalysts.

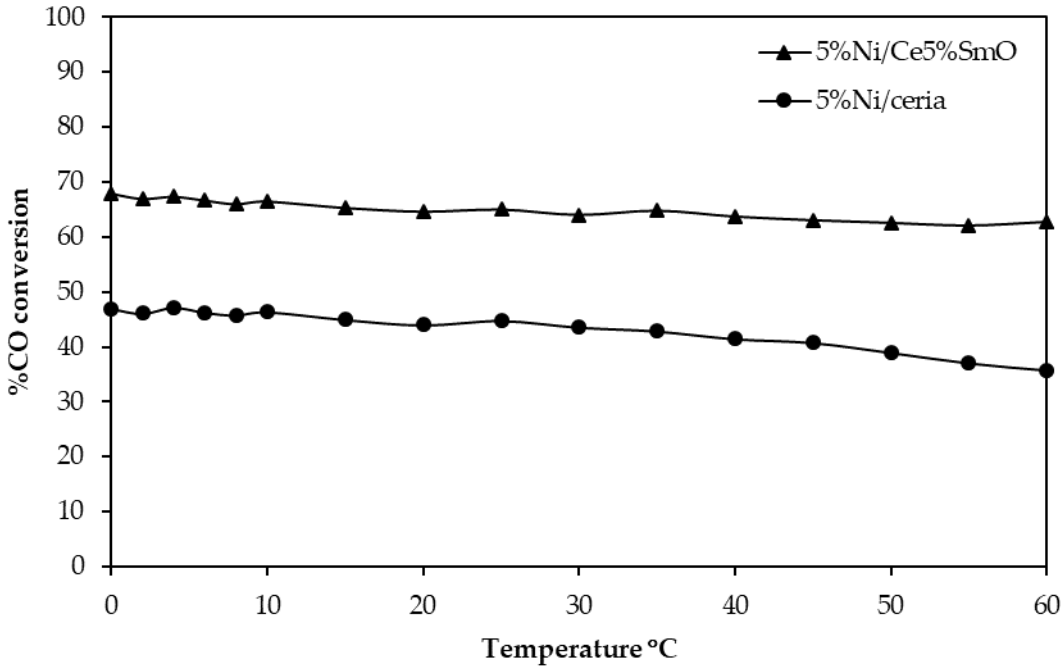

Figure 7. Long term stability test at 280 °C for supported Ni catalysts prepared by combustion method.

Thermogravimetric profiles (Figure 8) of the used 5%Ni/CeO_2 and 5%Ni/Ce5%SmO catalysts prepared by combustion method were further conducted for carbon deposits analysis. Relative weight was slightly enhanced between 400 and 550 °C, which may be contributed to by nickel oxidation to nickel oxide during the oxidative treatment. On the other hand, relative weight was quickly decreased between 550 and 720 °C, which was due to the oxidation of carbon deposits. Thermogravimetric analysis showed that 13% and 37% carbon was formed in the used 5%Ni/Ce5%SmO(combustion) and 5%Ni/CeO_2(combustion), respectively. Therefore, 5%Ni/Ce5%SmO catalyst provides lower carbon deposition after the water gas shift reaction test than the 5%Ni/CeO_2 catalyst, which is attribute to high stable performance and greater hydrogen production rates.

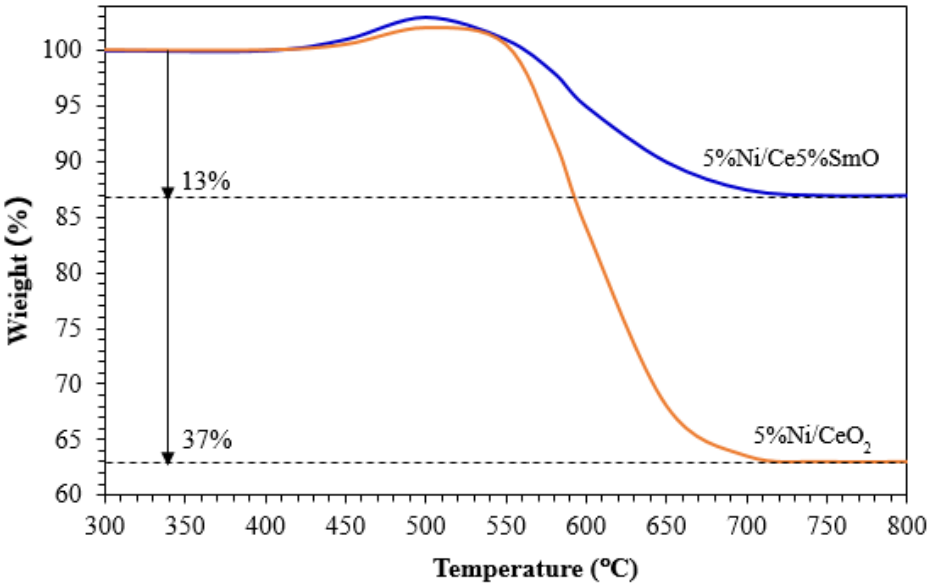

Figure 8. Thermogravimetric analysis of the used Ni catalysts prepared by combustion method.

The acidity of Ni/CeO_2 and Ni/Ce5%SmO catalysts prepared by combustion method was investigated by temperature programmed NH_3 desorption (NH_3-TPD) technique (Figure 9). Addition of Sm into $5\%Ni/CeO_2$ shifts the NH_3 desorption peak to a lower temperature. It means that the weak acid site increased by the addition of Sm to the support. The result of thermogravimetric analysis suggested that Ni/Ce5%SmO catalyst had less carbon deposition. Therefore, the increase of weak acid sites of the Ni/Ce5%SmO catalyst would decrease the carbon deposition due to them easily being removed.

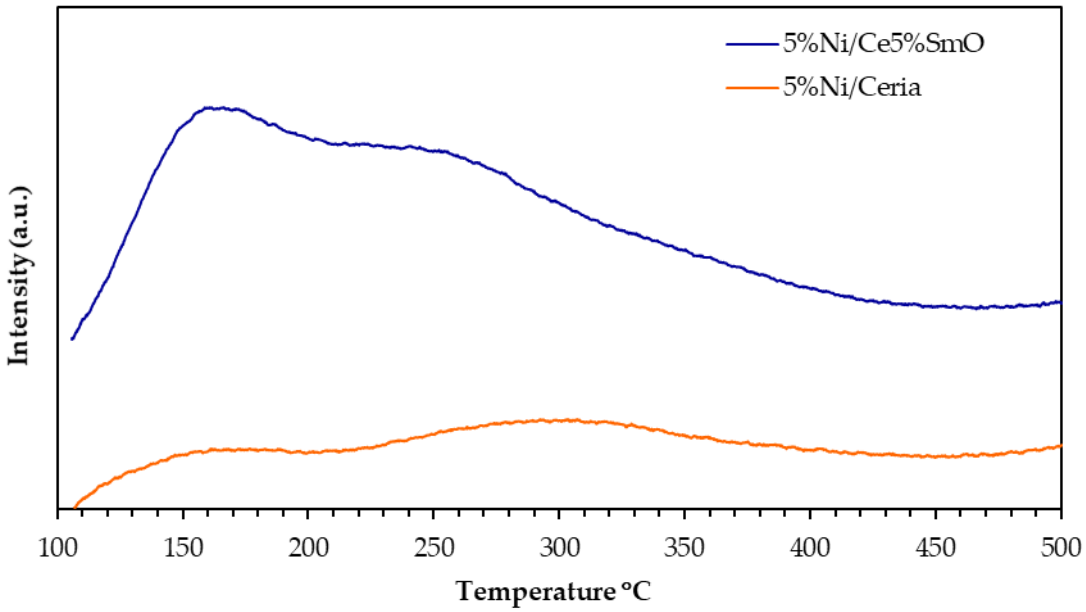

Figure 9. Temperature programmed NH_3 desorption profile of $5\%Ni/CeO_2$ and 5%Ni/Ce5%SmO catalysts prepared by combustion method.

The combination of NH_3-TPD with the water gas shift activity result indicated that surface acidity of the catalyst is beneficial for CO adsorption because a CO reactant is a weak base. Moreover, acidic character of the Ni catalyst surface facilitates CO_2 desorption, leaving free active sites for CO and H_2O adsorption in subsequent WGS reaction cycle. The desorbed NH_3 content was calculated from the NH_3desorption peak area. The NH_3 desorption peak area of Ni/Ce5%SmO is greater than that of Ni/CeO_2, which indicates that the acidity of Ni/Ce5%SmO was higher than Ni/CeO_2. Therefore, the increased acidity of Ni/Ce5%SmO enhances the amount of adsorbed CO on the catalyst surface, consequently increasing the water gas shift performance.

4. Conclusions

Ni/CeO_2 and Ni/CeSmO were synthesized with different preparation methods and Sm loading of 0–15 wt.%. Various preparation methods including combustion, sol gel and sol gel-combustion have been studied to improve the water gas shift performance of nickel catalysts. It was found that the promoted catalysts (Ni/CeSmO) exhibited greater catalytic activity than the unpromoted catalysts (Ni/ceria). Among all investigated catalysts, the one-step combustion method produced 5%Ni/Ce5%SmO catalyst with the highest activity in the water gas shift reaction. This related to high surface area and dispersion of metallic Ni, as more surface active sites are exposed to reactants. In addition, the increase of surface acidity of 5%Ni/Ce5%SmO prepared by combustion method accelerates CO adsorption consequently rising the water gas shift performance. Moreover, increasing the weak acid sites of Ni/Ce5%SmO catalyst prepared by combustion method would decrease the carbon deposition because it is easily removed. The enhancement of oxygen vacancy concentration of 5%Ni/Ce5%SmO synthesized by combustion method facilitates the redox process at the catalyst surface. These results are beneficial for H_2 production with high efficiency and the

long-term stability of the catalyst. The preparation of support by the combustion method is beneficial on the water gas shift reaction. Stronger interaction between Ni and CeO_2 is formed results in high Ni dispersion which could have helped in preventing the sintering of Ni–CeO_2. Moreover, the combustion method produced homogeneous, very fine and crystalline powders in a single step without the need of intermediate decomposition and calcining steps, which leads to reducing time for the support preparation.

Author Contributions: Conceptualization, P.T.; methodology, P.T.; validation, O.T. and P.T.; formal analysis, P.T.; investigation, P.T.; resources, O.T. and P.T.; data curation, P.T.; writing—original draft preparation, O.T. and P.T.; writing—review and editing, O.T. and P.T.; supervision, P.T.; funding acquisition, O.T. and P.T. All authors have read and agreed to the published version of the manuscript.

Funding: This research was funded by Faculty of Science and Technology, Thammasat University, Contract No. SciGR23/2565 and Thammasat University Research Unit in smart materials from biomass.

Institutional Review Board Statement: Not applicable.

Informed Consent Statement: Not applicable.

Data Availability Statement: Data will be made available on request.

Acknowledgments: The authors gratefully acknowledge the financial support provided by Faculty of Science and Technology, Thammasat University, Contract No. SciGR23/2565 and the Thammasat University Research Unit in smart materials from biomass.

Conflicts of Interest: The authors declare no conflict of interest.

References

1. Li, Y.; Fu, Q.; Flytzani-Stephanopoulos, M. Low-temperature water-gas shift reaction over Cu-and Ni-loaded cerium oxide catalysts. *Appl. Catal. B Environ.* **2000**, *27*, 179–191. [CrossRef]
2. Jacobs, G.; Chenu, E.; Patterson, P.M.; Williams, L.; Sparks, D.; Thomas, G.; Davis, B.H. Water-gas shift: Comparative screening of metal promoters for metal/ceria systems and role of the metal. *Appl. Catal. A Gen.* **2004**, *258*, 203–214. [CrossRef]
3. Czekaj, I.; Loviat, F.; Raimondi, F.; Wambach, J.; Biollaz, S.; Wokaun, A. Characterization of surface processes at the Ni-based catalyst during the methanation of biomass-derived synthesis gas: X-ray photoelectron spectroscopy (XPS). *Appl. Catal. A Gen.* **2007**, *329*, 68–78. [CrossRef]
4. Lomonaco, J.G.; Tojira, O.; Charojrochkul, S.; Tepamatr, P. Structure-activity relationship of ceria based catalyst for hydrogen production. *Chiang Mai J. Sci.* **2022**, *49*, 1129–1134. [CrossRef]
5. Tojira, O.; Lomonaco, J.G.; Sesuk, T.; Charojrochkul, S.; Tepamatr, P. Enhancement of hydrogen production using Ni catalysts supported by Gd-doped ceria. *Heliyon* **2021**, *7*, e08202. [CrossRef] [PubMed]
6. Si, R.; Tao, J.; Evans, J.; Park, J.B.; Barrio, L.; Hanson, J.C.; Zhu, Y.; Hrbek, J.; Rodriguez, J.A. Effect of ceria on gold–titania catalysts for the water–gas shift reaction: Fundamental studies for Au/CeOx/TiO_2(110) and Au/CeOx/TiO_2 Powders. *J. Phys. Chem. C* **2012**, *116*, 23547–23555. [CrossRef]
7. Ro, I.; Resasco, J.; Christopher, P. Approaches for understanding and controlling interfacial effects in oxide-supported metal catalysts. *ACS Catal.* **2018**, *8*, 7368–7387. [CrossRef]
8. Tepamatr, P.; Buarod, E.; Laosiripojana, N.; Charojrochkul, S. Study of water gas shift reaction over ceria based catalysts in solid oxide fuel cells. *ECS Trans* **2015**, *68*, 1207–1217. [CrossRef]
9. McFarland, E.W.; Metiu, H. Catalysis by Doped Oxides. *Chem. Rev.* **2013**, *113*, 4391–4427. [CrossRef]
10. AlKhoori, A.A.; Polychronopoulou, K.; Belabbes, A.; Jaoude, M.A.; Vega, L.F.; Sebastian, V.; Hinder, S.; Baker, M.A.; Zedan, A.F. Cu, Sm co-doping effect on the CO oxidation activity of CeO_2. A combined experimental and density functional study. *Appl. Surf. Sci.* **2020**, *521*, 146305. [CrossRef]
11. Zagaynov, I.V.; Shelepin, I.V.; Fedorov, S.V.; Naumkin, A.V.; Bykov, A.V.; Konovalov, A.A. Sm(Nd) doped ceria materials for multifunctional application. *Ceram. Int.* **2021**, *47*, 22201–22208. [CrossRef]
12. Meshkani, F.; Rezaei, M. Preparation of mesoporous chromium promoted magnetite based catalysts for high temperature water gas shift reaction. *Ind. Eng. Chem. Res.* **2015**, *54*, 1236–1242. [CrossRef]
13. Reddy, B.M.; Thrimurthulu, G.; Katta, L. Design of efficient $Ce_xM_{1-x}O_{2-\delta}$ (M = Zr, Hf, Tb and Pr) nanosized model solid solutions for CO oxidation. *Catal. Lett.* **2011**, *141*, 572–581. [CrossRef]
14. Krishna, K.; Bueno-López, A.; Makkee, M.; Moulijn, J.A. Potential rare-earth modified CeO_2 catalysts for soot oxidation. Part III. Effect of dopant loading and calcination temperature on catalytic activity with O_2 and NO + O_2. *Appl. Catal. B Environ.* **2007**, *75*, 210–220. [CrossRef]

15. Neelapala, S.D.; Dasari, H. Catalytic soot oxidation activity of Cr-doped ceria (Ce Cr $O_{2-\delta}$) synthesized by sol-gel method with organic additives. *Mater. Sci. Energy Technol.* **2018**, *1*, 155–159. [CrossRef]
16. Jazayeri, S.H.; Bondioli, F.; Salem, S.; Allahverdi, A.; Shirvani, M.; Ferrari, A.M. Effect of pH, molar ratio of fuel to nitrates and calcination temperature on the glycine-nitrate synthesis of nano $CoAl_2O_4$. *Adv. Sci. Technol.* **2010**, *68*, 176–181.
17. Prasad, H.D.; Son, J.; Kim, B.; Lee, H.; Lee, J. A significant enhancement in sintering activity of nanocrystalline Ce0.9Gd0.1O1.95 powder synthesized by a glycine-nitrate-process. *J. Ceram. Process. Res.* **2010**, *11*, 176–183.
18. Marinho, A.L.A.; Rabelo-Neto, R.C.; Epron, F.; Bion, N.; Toniolo, F.S.; Noronha, F.B. Embedded Ni nanoparticles in $CeZrO_2$ as stable catalyst for dry reforming of methane. *Appl. Catal. B Environ.* **2020**, *268*, 118387. [CrossRef]
19. Hwang, C.C.; Huanga, T.H.; Tsai, J.S.; Lin, C.; Peng, C.H. Combustion synthesis of nanocrystalline ceria (CeO_2) powders by a dry route. *Mater. Sci. Eng. B.* **2006**, *132*, 229–238. [CrossRef]
20. Chinarro, E.; Jurado, J.R.; Colomer, M.T. Synthesis of ceria-based elecrtolyte nanometric powders by urea–combustion technique. *J. Eur. Ceram. Soc.* **2007**, *27*, 3619–3623. [CrossRef]
21. Tokeda, T.; Kato, K.; Kikkawa, S. Gel combustion synthesis of rare earth aluminate using glycine or urea. *J. Ceram. Soc. Jpn.* **2007**, *115*, 588–591. [CrossRef]
22. Tepamatr, P.; Laosiripojana, N.; Sesuk, T.; Charojrochkul, S. Effect of samarium and praseodymium addition on water gas shift performance of Co/CeO_2 catalysts. *J. Rare Earths* **2020**, *38*, 1201–1206. [CrossRef]
23. Tepamatr, P.; Laosiripojana, N.; Charojrochkul, S. Water gas shift reaction over monometallic and bimetallic catalysts supported by mixed oxide materials. *Appl. Catal. A: Gen.* **2016**, *523*, 255–262. [CrossRef]
24. Tan, J.; Lee, D.; Ahn, J.; Kim, B.; Kim, J.; Moon, J. Thermally driven in situ exsolution of Ni nanoparticles from (Ni, Gd) CeO_2 for high-performance solid oxide fuel cells. *J. Mater. Chem.* **2018**, *6*, 18133–18142. [CrossRef]
25. Tada, S.; Shimizu, T.; Kameyama, H.; Haneda, T.; Kikuchi, R. Ni/CeO_2 catalysts with high CO_2 methanation activity and high CH_4 selectivity at low temperatures. *Int. J. Hydrogen Energy* **2012**, *37*, 5527–5531. [CrossRef]
26. Zhou, G.; Liu, H.; Cui, K.; Jia, A.; Hu, G.; Jiao, Z.; Liu, Y.; Zhang, X. Role of surface Ni and Ce species of Ni/CeO_2 catalyst in CO_2 methanation. *Appl. Surf. Sci.* **2016**, *383*, 248–252. [CrossRef]
27. Ding, M.; Tu, J.; Zhang, Q.; Wang, M.; Tsubaki, N.; Wang, T.; Ma, L. Enhancement of methanation of bio-syngas over CeO_2-modified Ni/Al_2O_3 catalysts. *Biomass Bioenergy* **2016**, *85*, 12–17. [CrossRef]
28. Wang, L.H.; Zhang, S.X.; Liu, Y.A. Reverse water gas shift reaction over Co–precipitated Ni–CeO_2 catalysts. *J. Rare Earths* **2008**, *26*, 66–70. [CrossRef]
29. Odedairo, T.; Chen, J.; Zhu, Z. Metal–support interface of a novel Ni–CeO_2 catalyst for dry reforming of methane. *Catal. Commun.* **2013**, *31*, 25–31. [CrossRef]
30. Lee, Y.L.; Jha, A.; Jang, W.J.; Shim, J.O.; Jeon, K.W.; Na, H.S.; Kim, H.M.; Lee, D.W.; Yoo, S.Y.; Jeon, B.H.; et al. Optimization of cobalt loading in Co–CeO_2 catalyst for the high temperature water–gas shift reaction. *Top. Catal.* **2017**, *60*, 721–726. [CrossRef]
31. Goerke, O.; Pfeifer, P.; Schubert, K. Water gas shift reaction and selective oxidation of CO in microreactors. *Appl. Catal. A Gen.* **2004**, *263*, 11–18. [CrossRef]